# Ancilla-free scheme of deterministic topological quantum gates for Majorana qubits

Su-Qi Zhang,[1,2] Jian-Song Hong,[3] Yuan Xue [ORCID],[4] Xun-Jiang Luo,[1,2] Li-Wei Yu,[5] Xiong-Jun Liu,[3,6,7,8,*] and Xin Liu [ORCID][1,2,8,†]

[1]*School of Physics and Institute for Quantum Science and Engineering, Huazhong University of Science and Technology,*
*Wuhan, Hubei 430074, China*
[2]*Wuhan National High Magnetic Field Center and Hubei Key Laboratory of Gravitation and Quantum Physics, Wuhan, Hubei 430074, China*
[3]*International Center for Quantum Materials and School of Physics, Peking University, Beijing 100871, China*
[4]*Department of Physics, The University of Texas at Austin, Austin, Texas 78705, USA*
[5]*Theoretical Physics Division, Chern Institute of Mathematics and LPMC, Nankai University, Tianjin 300071, China*
[6]*International Quantum Academy, Shenzhen 518048, China*
[7]*CAS Center for Excellence in Topological Quantum Computation, University of Chinese Academy of Sciences, Beijing 100190, China*
[8]*Hefei National Laboratory, Hefei 230088, China*

The realization of quantum gates in topological quantum computation still confronts significant challenges in both fundamental and practical aspects. Here, we propose an ancilla-free, deterministic, and topologically protected measurement-based scheme to realize the implementation of Clifford quantum gates on the Majorana qubits. Our scheme is based on a rigorous proof that the single-qubit gate can be performed by leveraging the neighboring Majorana qubit but not disturbing its carried quantum information, enabling an ancilla-free scheme for the topological quantum computing with Majorana qubits. Benefiting from the ancilla-free construction, we show the minimum measurement sequences with four steps to achieve two-qubit Clifford gates by constructing their geometric visualization. The uncertainty of the current strategy can be avoided by manipulating the Majorana modes in their parameter space, as shown in a concrete Majorana platform, correcting the undesired measurement outcomes while maintaining topological protection. Our scheme identifies the minimal operations of measurement-based topological and deterministic Clifford gates and offers an ancilla-free design of topological quantum computation.

## I. INTRODUCTION

Majorana zero modes (MZMs) obey exotic non-Abelian braiding statistics, making them of great interest in fundamental physics and the potential application to topological quantum computation (TQC) [1–5]. Braiding two MZMs physically by moving one around the other in real space is theoretically straightforward [6–13] but challenging to experimental implementation [14–40]. Measurement-based schemes provide an alternative method to realize the braiding transformations without physically moving Majorana modes [41–44]. However, a comprehensive understanding of realizing the Clifford gates in the measurement-based schemes is still lacking. So far the measurement-based schemes necessitate ancillary MZMs to implement the topological quantum gates. In comparison, an ancilla-free scheme can potentially have great advantages in saving resources, simplifying the design of quantum gates, and providing more theoretical insights. However, whether such a scheme exists was unknown.

In this paper, we prove the sufficiency and efficiency of using two Majorana qubits, without the need for ancillary MZMs or qubits, to implement single- and two-qubit Clifford gates through a measurement-based scheme in a deterministic manner. Firstly, we show a key result that the implementation of a single-qubit gate can be achieved by using a neighboring Majorana qubit but not disturbing its carried quantum information, eliminating the requirement for ancillary MZMs in Majorana-based TQC design. By leveraging the benefits of the ancilla-free construction, we propose the minimal scheme of implementing two-qubit Clifford gates and show rigorously the minimum measurement sequences involve only four steps through a geometric visualization. Further, through a diagrammatic formalism, we demonstrate that Pauli gate [45–47] can be applied to our scheme to correct undesired outcomes by manipulating the MZMs in their parameter space, yielding the deterministic Clifford gates with topological protection. Finally, we showcase the experimental accessibility of our proposal by demonstrating its applicability in a concrete Majorana platform.

## II. SINGLE-QUBIT GATE IMPLEMENTATION WITH TWO TOPOLOGICAL QUBITS

To perform quantum gate operation with Majorana qubits, the essential task is to exchange two MZMs. The measurement-only method provides a means to braid MZMs without physical movement, but it requires a larger Hilbert space to facilitate the teleportation, rather than the collapse, of

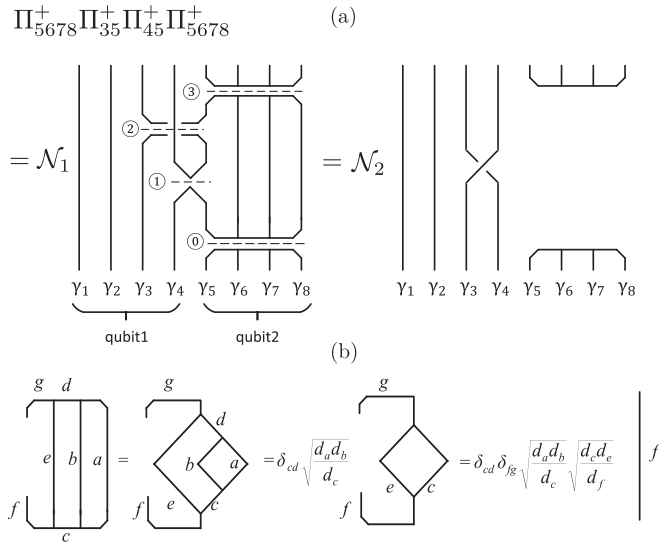*xiongjunliu@pku.edu.cn
†phyliuxin@hust.edu.cn

FIG. 1. Braiding $\gamma_3$ and $\gamma_4$ within two qubits. (a) The time direction is vertical from bottom to top in our representation and $\mathcal{N}_i$ is the normalization factor. $\gamma_{i=1-8}$ is the $i$th MZM from left to right. The dashed line with the circle $j$ marks the $j$th measurement. (b) The locality principle is detailed in (a) for qubit2. The letters $a-g$ are the labels of anyons, $d_a$ is the quantum dimension of $a$, and so forth.

quantum information [41,43,44]. Starting with two Majorana qubits provides an advantage as the eight MZMs offer sufficient redundancy to teleport quantum information initially stored on the computational basis. In contrast, when beginning with only one Majorana qubit, a pair of ancillary MZMs is required to introduce the necessary redundancy. This suggests that we may braid two MZMs in one qubit with the help of the MZMs in the neighbor qubit. However, when attempting to braid two MZMs in one qubit with the help of the neighboring qubit, a crucial question arises: Is it fundamentally allowed without changing the stored quantum information, even if the neighboring qubit can possess arbitrary quantum information and may be entangled with additional qubits? Fortunately, the answer is affirmative, and it can be rigorously proven using the isotopy invariant diagrammatic formalism [41,48–51].

We start from eight Majorana zero modes, the minimal requirement to constructing two Majorana qubits with sparse encoding [52]. The first and last four modes form the first and second Majorana qubits, respectively [Fig. 1(a)]. Throughout our paper, the total fermion parity of the eight MZMs remains even. Initially, the quantum information is stored in the computational space where each qubit shares even parity, denoted as $\hat{P}_{1234(5678)} = -\gamma_{1(5)}\gamma_{2(6)}\gamma_{3(7)}\gamma_{4(8)} = +1$. This even parity is guaranteed by the four MZMs measurement, $\Pi^+_{1234(5678)} = (1 + \hat{P}_{1234(5678)})/2$ [Fig. 1(a)]. Here and after, we define the fermion parity and measurement operators as $\hat{P}_{i_1...i_n}$ and $\Pi^\pm_{i_1...i_n} = (1 \pm \hat{P}_{i_1...i_n})/2$ of the $n$ MZMs. Without loss of generality, we first attempt to braid MZMs $\gamma_3$ and $\gamma_4$ in the first qubit with the assistance of the second qubit. The scheme comprises three successive nondestructive topological charge projective measurements ($\Pi^+_{45}$, $\Pi^+_{35}$, and $\Pi^+_{5678}$), as shown in the left-hand side of the diagrammatic representation of Fig. 1(a). Note that although the the measurement operations $\Pi^+_{45}$ and $\Pi^+_{35}$ result in the teleportation of quantum states to $\hat{P}_{1234} = -1$ subspace, we require the degeneracy of $\hat{P}_{1234} = \pm 1$ subspaces to ensure the topological protection. After the quantum gate operation, we lift the degeneracy. Tuning the degeneracy between even and odd Hilbert spaces can be achieved by tuning the Josephson coupling between two Majorana qubits, which is demonstrated in our setup discussion. Remarkably, the strands in qubit-2 can be simplified through the locality principle [Fig. 1(b)] into one strand. Meanwhile, the isotopy invariance allows us to freely stretch or slide around a strand so long as its topology remains fixed. After stretching the lines in Fig. 1(a), it is clear that the three successive measurements are equivalent to exchange $\gamma_3$ and $\gamma_4$ in qubit-1 and perform identity operation in qubit-2. Thus, we rigorously prove that the exchange of two MZMs in one qubit can be achieved with the assistance of the neighboring qubit but not affecting its quantum information.

## III. MINIMAL MEASUREMENT-BASED SCHEME OF CONTROLLED-Z GATE

Without loss of generality, we first consider the controlled-Z (CZ) gate with the first and second qubits as control and target, respectively. Unlike the $\pi/4$-gate, the CZ gate lacks a standard diagrammatic representation, making it difficult to visualize. For example, we have found that the sequence of four times measurements $\Pi^+_{5678}\Pi^+_{35}\Pi^+_{34}\Pi^+_{46}$ can implement the CZ gate in our ancilla-free Majorana qubits through direct calculations. We can make a hindsight demonstration through the continuous deformation of its diagrammatic representation into the celebrated proposal [52], which involves two measurements and three exchange operations in an eight MZMs system [Fig. 2(a)]. But this deformation is case by case and lacks a general rule to follow. Recent studies have discovered many measurement sequences to implement the same CZ gate for two Majorana qubits with one or two pairs of ancillary MZMs. It has been shown by brute force that four measurements are the minimum required to realize the CZ gate, but the principles behind these sequences are still unclear [53]. Furthermore, these measurement sequences involve teleporting quantum states in ten or twelve MZMs Hilbert spaces, which cannot be applied to ancillary-free two Majorana qubits with only eight MZMs. As a result, there is currently no general measurement-based construction method for CZ gates of topological qubits.

To address these issues, we propose a solution based on the ancillary-free two Majorana qubits system. By preserving the even total fermion parity, the measurements teleport the quantum states in eight-dimensional (8D) Hilbert space, which can be decomposed into the direct sum of the four-dimensional computational and noncomputational spaces [upper gray plane and lower blue plane in Fig. 2(b)] stabilized by the stabilizers $\{\hat{P}^+_{1-8}, \pm\hat{P}^+_{5678}\}$ respectively. We define the qubit basis in computational basis as

$$\Psi = \{\psi_1, \psi_2, \psi_3, \psi_4\} = \{|0000\rangle, |0011\rangle, |1100\rangle, |1111\rangle\}.$$

To avoid collapsing the quantum information, the first measurement $\Pi^+_I$ must teleport the states in a redundant Hilbert space. Therefore, we choose the parity operator $\hat{P}_I$ for the
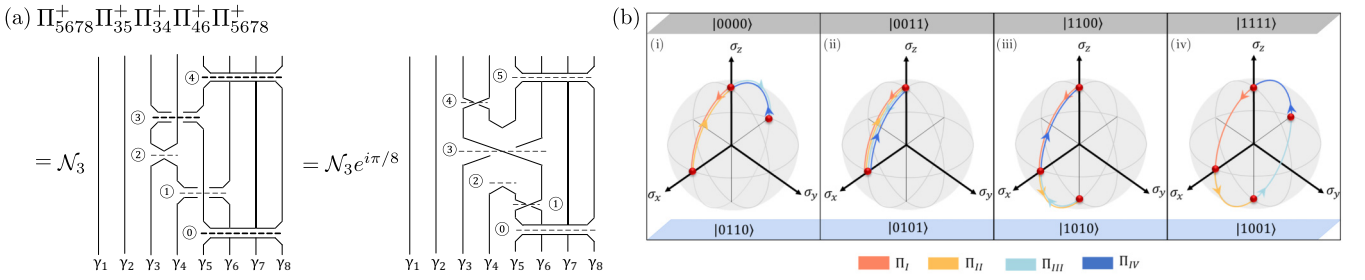
FIG. 2. CZ gate. (a) Diagrammatic representation of measurement-based CZ gate. (b) Geometric visualization of measurement-based CZ gate in Bloch spheres, with consistent measurement sequences in (a). The upper gray (and lower blue) planes correspond to computational and noncomputational spaces, respectively. The colored paths indicate the equivalent measurements.

first measurement to anticommute with $\hat{P}_{5678}$. WLoG, we take $\hat{P}_I = \hat{P}_{46}$. The states $\hat{P}_{46}\Psi = \Pi_{46}^+\{\psi_1, \psi_2, \psi_3, \psi_4\}$ expand the noncomputational spaces. To visualize the computational and noncomputational Hilbert space, we define the states $\Psi$ and $\hat{P}_{46}\Psi$ as the north and south poles of the four Bloch spheres in which the states $\Pi_{46}^+\Psi$ lie along the $+x$ axis in each Bloch sphere [Fig. 2(b)]. In this case, the parity operator $\hat{P}_{5678(46)}$ in the four Bloch spheres take the form diag$\{\sigma_{z(x)}, \sigma_{z(x)}, \sigma_{z(x)}, \sigma_{z(x)}\}$. Since the CZ gate is diagonal in the computational basis, its measurement sequences should teleport within each Bloch sphere. Consequently, the quantum teleportation through each projective measurement is equivalent to the adiabatic evolution of the states along the 1/4 great circle connecting the projective points at the Bloch sphere [Fig. 2(b)]. Performing the measurement sequences on each qubit basis is equivalent to a unitary evolution in the corresponding Bloch sphere along a closed geodesic, accumulating a geometric phase in each basis. To achieve the CZ gate, the state $|1111\rangle$ must acquire a $\pi$ phase [Fig. 2(b)(iv)], which requires the last Bloch sphere's state teleportation to follow a great circle passing through the north and south poles. We can choose $\Pi_{II} = (1 + \hat{P}_{34})/2$ with $\hat{P}_{34} = $ diag$\{\sigma_z, \sigma_z, -\sigma_z, -\sigma_z\}$ and $\Pi_{III} = (1 + \hat{P}_{35})/2$ with $\hat{P}_{III} = $ diag$\{-\sigma_x, \sigma_x, \sigma_x, -\sigma_x\}$. Apparently, the projective measurement $\Pi_{II(III)}$ leads the states in different Bloch spheres to undergo different paths, with only the last Bloch sphere's path being a great circle. Therefore, the CZ gate implemented through the measurements $\Pi_{5678}^+\Pi_{35}^+\Pi_{34}^+\Pi_{46}^+$ without additional ancillary MZMs can be visualized by the paths along the geodesics [Fig. 2(b)]. Furthermore, as each teleportation corresponds to the adiabatic evolution of 1/4 great circle [54], a minimum of four teleportations are needed to implement the CZ gate. We have identified 16 different four-times measurement sequences to implement the CZ gate by varying the choices of $\hat{P}_I$. Additionally, we have also determined eight sequences for the iCZ gate, diag$\{1, 1, i, -i\}$. These diverse sequences offer flexibility in constructing two-qubit gates for various experimental platforms (see the Supplemental Material, SM [55]).

## IV. DETERMINISTIC TOPOLOGICAL GATES WITH CORRECTION

In the measurement-based scheme, undesired outcomes are inevitable. Pauli tracking method [47,53] provides a practical

way to avoid physical corrections when performing Clifford gates. However, the generic quantum circuits with Majorana qubits inevitably have nontopologically protected gates. The interplay between the generic quantum circuits and Pauli tracking method may lead unforeseen error evolution and propagation [56]. Therefore, it is worthwhile to propose a scheme to implement physical corrections with topological protection.

According to the fusion and braiding rules, the different fusion channels can be connected using the following equation:

$$\sum_{j,k}(F_{abc}^{d\ -1})_j^k (R_{bc}^j)^2 (F_{abc}^d)_i^j$$

(1)

where $(F_{abc}^d)_j^i$ and $R_{ab}^j$ are the fusion and exchange matrices respectively and $a(b, c, d)$ represent the non-Abelian anyons and $i(j, k)$ their fusion channels. The full braiding of two $Z_{2m}$ parafermions, according to the spin-statistics theorem [57,58], follows $R^2 \propto e^{isn^2\pi/m}$ with $s \in \mathbb{Z}$, $n$ corresponds to the topological charge and $2m$ the number of fusion channels. For Ising anyons ($s = 1$ and $m = 1$) with two fusion channels (vacuum and fermion), denoted by $n = 0$ and $n = 1$ respectively, the pentagon and hexagon identities yield $\sum_j(F_{abc}^{d\ -1})_j^k (R_{ab}^j)^2 (F_{abc}^d)_i^j = e^{-i\pi/4}\sigma_{ik}^x$, where $\sigma^x$ acts on the fusion space of $\gamma_a$ and $\gamma_b$. Simplifying Eq. (1), we have

$$= e^{i\frac{\pi}{4}} \qquad , \qquad = e^{-i\frac{\pi}{4}}$$

(2)

with $v$ and $f$ the fusion channels of vacuum and fermion. Note that each diagram in the above is a quantum state. Thus the corresponding projector operator satisfies
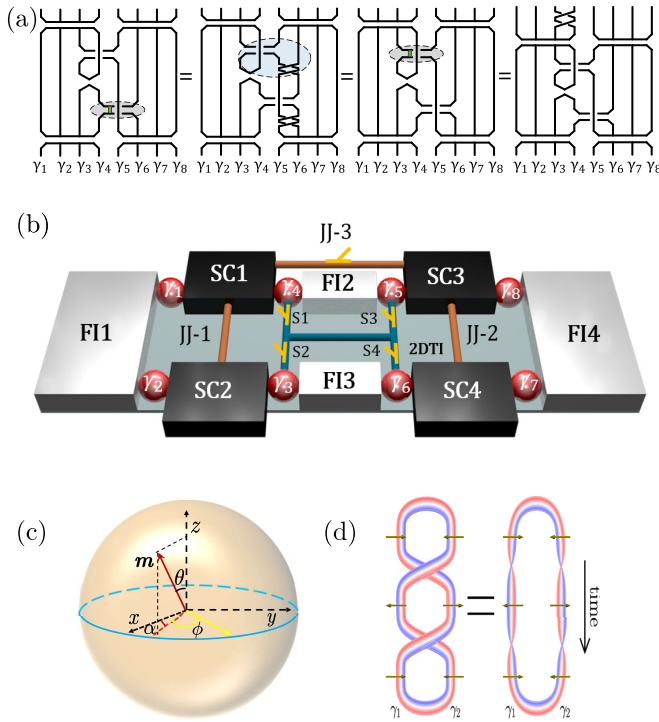
$$f \qquad = $$

(3a)

FIG. 3. (a) A demonstration of propagating undesired outcome in the sequence $\Pi_{5678}^{(+1)}\Pi_{35}^{(+1)}\Pi_{34}^{(+1)}\Pi_{46}^{(-1)}\Pi_{5678}^{(+1)}$ through the full braiding transformation. The small solid-green squares mark the measurements as nonvacuum, and dashed-gray and blue circles mark the deformations. (b) Two Majorana qubits from the SC/2DTI/FI hybrid system. (c) The relations among the Majorana spin in FI region (yellow arrow), magnetization (red arrow) and SOC field direction ($\boldsymbol{e}_z$). The polar and azimuth angles of FI magnetization are $\theta$ and $\alpha$, respectively. The Majorana spin lies in the $x$-$y$ plane with azimuth angle $\phi$. (d) The equivalence between braiding two MZMs and twisting each Majorana spin by $2\pi$. The arrows indicate the MZM spin.

$$f \quad \Bigg| \quad = \quad \Bigg| \qquad (3b)$$

We find that the transformation of undesired outcomes to desired outcomes using Eqs. (3a) and (3b) within the framework of full isotopy formalism can be achieved in different ways: The former adds the additional braiding operations as the payment; the latter transports the exchange operations occurring before the measurement to after the measurement. By combining these two equations and the full isotopy formalism, we can convert all the fermion measurement results to the vacuum while transferring the additional braiding operations after the final measurement. In Fig. 3(a), we demonstrate how to propagate undesired outcomes, taking the example of an undesired outcome at the first measurement of the CZ gate (i.e., $\Pi_{5678}^+\Pi_{35}^+\Pi_{34}^+\Pi_{46}^-\Pi_{5678}^+$, detailed deformation version available in the SM [55]). Taking Eqs. (3a) and (3b) (dashed-gray and blue circles) in succession, the undesired

outcome shifts along the time axis from the first to the third measurement [the third diagram in Fig. 3(a)]. Repeating the similar procedure with Eq. (3a), the consequences with undesired measurement outcome are transformed to the desired one with additional full braiding operations, which ends up with a full braiding of $\gamma_3$ and $\gamma_4$. Therefore, we only need to eliminate the full braiding by imposing an opposite braiding. Such a full braiding for correction can be achieved by parameter control or measurements, as discussed below.

## V. A CONCRETE EXAMPLE

We demonstrate our ancilla-free scheme and correction through a concrete Majorana platform, consisting of a superconductor (SC), a two-dimensional topological insulator (2DTI), and a ferromagnetic insulator (FI) [Fig. 3(b)]. The low energy BdG Hamiltonian in spinor basis $\hat{c}(\boldsymbol{r}) = [c_\uparrow(\boldsymbol{r}), c_\downarrow(\boldsymbol{r}), c_\downarrow^\dagger(\boldsymbol{r}), -c_\uparrow^\dagger(\boldsymbol{r})]^T$ takes

$$\hat{H} = \begin{pmatrix} h(\hat{p}) + \boldsymbol{m}(\boldsymbol{r}) \cdot \sigma & \Delta_{\mathrm{SC}}(\boldsymbol{r})e^{-i\varphi(\boldsymbol{r})} \\ \Delta_{\mathrm{SC}}(\boldsymbol{r})e^{i\varphi(\boldsymbol{r})} & -h(\hat{p}) + \boldsymbol{m}(\boldsymbol{r}) \cdot \sigma \end{pmatrix}, \qquad (4)$$

where $\sigma_{x,y,z}$ are Pauli matrices in spin space, $h(\hat{\boldsymbol{p}}) = v_\mathrm{f}\hat{p}\sigma_z - \mu$, with $v_\mathrm{f}$ the Fermi velocity of edge states, and $\mu$ the chemical potential, $\Delta(\boldsymbol{r})$ is the proximity induced $s$-wave SC gap amplitude with SC phase $\varphi(\boldsymbol{r})$ and $\boldsymbol{m}(\boldsymbol{r})$ is the proximity induced exchange field. Here $\varphi(\boldsymbol{r})$ gives the superconducting phase of each SC island. Each SC/FI interface supports one MZM.

We construct the Majorana qubits by connecting SC1 (SC3) and SC2 (SC4) via a Josephson junction JJ-1(JJ-2). Owing to the substantial Josephson coupling energy, they essentially function as a unified superconducting island, denoted as SC12 (SC34). The islands SC12 and SC34 are isolated when JJ-3 is off, so they form two independent Majorana qubits [44,59]. The fermion parity even states ($|e\rangle_{12}$, $|e\rangle_{34}$) on each island are the qubit states, which are gapped from odd subspace ($|o\rangle_{12}$, $|o\rangle_{34}$) by the charging energy(see the SM [55]). During single- or two-qubit gate operations, prior to measurement, we activate the JJ-3, amalgamating SC12 and SC34 into a larger superconducting island. This action induces the requisite degeneracy between $|e\rangle_{12} \otimes |e\rangle_{34}$ and $|o\rangle_{12} \otimes |o\rangle_{34}$. We turn off the coupling of JJ-3 after gate operations. The two-MZMs fermion parities can be measured by observing supercurrent direction in the lead linking two MZMs (see the SM [55]) [the blue bridge in Fig. 3(b)]. The four-MZMs measurement is performed through the dispersive readout (see the SM [55]).

The Majorana evolution in parameter space is equivalent to a full braiding, which provides the basis for experimental implementation of corrections. In particular, as the direction of magnetization $\boldsymbol{m}$ completes a closed trajectory enclosing the spin-orbit ($z$) axis, the Majorana wave functions span $2\pi$ solid angle in the Bloch sphere [Fig. 3(c)]. This results in a $\pi$ monodromy phase, corresponding to a full braiding operation of $\exp(-\pi\gamma_1\gamma_2/2)$ [60] as depicted in Fig. 3(d). The quantization of the monodromy phase is homotopy to the winding number of the magnetization around the SOC axis. Thus this operation is topologically protected. Similarly, winding the superconducting phase also introduces the quantized

monodromy phase $n\pi$ into the MZM (see the SM [55]). Therefore, the correction through braiding of MZMs can be achieved by manipulating them in either spin or phase parameter space with full topological protection.

## VI. CONCLUSIONS

We have proposed an ancilla-free measurement-based scheme to implement Clifford quantum gates with full topological protection. This design enables us to identify the minimal measurement sequences and allows the systematic construction of Clifford gates. Additionally, the deterministic quantum gates can be achieved through fully braiding Majorana modes in parameter space with topological protection.

Our study provides valuable insight into the optimal design for topological quantum computation.

[1] A. Y. Kitaev, Phys. Usp. **44**, 131 (2001).

[2] D. A. Ivanov, Phys. Rev. Lett. **86**, 268 (2001).

[3] C. Nayak, S. H. Simon, A. Stern, M. Freedman, and S. Das Sarma, Rev. Mod. Phys. **80**, 1083 (2008).

[4] N. Read and D. Green, Phys. Rev. B **61**, 10267 (2000).

[5] O. Motrunich, K. Damle, and D. A. Huse, Phys. Rev. B **63**, 224204 (2001).

[6] J. Alicea, Y. Oreg, G. Refael, F. von Oppen, and M. P. A. Fisher, Nat. Phys. **7**, 412 (2011).

[7] X.-J. Liu, C. L. M. Wong, and K. T. Law, Phys. Rev. X **4**, 021018 (2014).

[8] J. D. Sau, D. J. Clarke, and S. Tewari, Phys. Rev. B **84**, 094505 (2011).

[9] B. van Heck, A. R. Akhmerov, F. Hassler, M. Burrello, and C. W. J. Beenakker, New J. Phys. **14**, 035019 (2012).

[10] T. Hyart, B. van Heck, I. C. Fulga, M. Burrello, A. R. Akhmerov, and C. W. J. Beenakker, Phys. Rev. B **88**, 035121 (2013).

[11] L.-H. Wu, Q.-F. Liang, and X. Hu, Sci. Technol. Adv. Mater. **15**, 064402 (2014).

[12] B. van Heck, T. Hyart, and C. W. J. Beenakker, Phys. Scr. **2015**, 014007 (2015).

[13] X. Liu, X. Li, D.-L. Deng, X.-J. Liu, and S. Das Sarma, Phys. Rev. B **94**, 014511 (2016).

[14] V. Mourik, K. Zuo, S. M. Frolov, S. R. Plissard, E. P. A. M. Bakkers, and L. P. Kouwenhoven, Science **336**, 1003 (2012).

[15] M. T. Deng, C. L. Yu, G. Y. Huang, M. Larsson, P. Caroff, and H. Q. Xu, Nano Lett. **12**, 6414 (2012).

[16] L. P. Rokhinson, X. Liu, and J. K. Furdyna, Nat. Phys. **8**, 795 (2012).

[17] A. Das, Y. Ronen, Y. Most, Y. Oreg, M. Heiblum, and H. Shtrikman, Nat. Phys. **8**, 887 (2012).

[18] M.-X. Wang, C. Liu, J.-P. Xu, F. Yang, L. Miao, M.-Y. Yao, C. L. Gao, C. Shen, X. Ma, X. Chen *et al.*, Science **336**, 52 (2012).

[19] H. O. H. Churchill, V. Fatemi, K. Grove-Rasmussen, M. T. Deng, P. Caroff, H. Q. Xu, and C. M. Marcus, Phys. Rev. B **87**, 241401(R) (2013).

[20] J.-P. Xu, C. Liu, M.-X. Wang, J. Ge, Z.-L. Liu, X. Yang, Y. Chen, Y. Liu, Z.-A. Xu, C.-L. Gao, D. Qian, F.-C. Zhang, and J.-F. Jia, Phys. Rev. Lett. **112**, 217001 (2014).

[21] S. Nadj-Perge, I. K. Drozdov, J. Li, H. Chen, S. Jeon, J. Seo, A. H. MacDonald, B. A. Bernevig, and A. Yazdani, Science **346**, 602 (2014).

[22] W. Chang, S. M. Albrecht, T. S. Jespersen, F. Kuemmeth, P. Krogstrup, J. Nygård, and C. M. Marcus, Nat. Nanotechnol. **10**, 232 (2015).

[23] H.-H. Sun, K.-W. Zhang, L.-H. Hu, C. Li, G.-Y. Wang, H.-Y. Ma, Z.-A. Xu, C.-L. Gao, D.-D. Guan, Y.-Y. Li, C. Liu, D. Qian, Y. Zhou, L. Fu, S.-C. Li, F.-C. Zhang, and J.-F. Jia, Phys. Rev. Lett. **116**, 257003 (2016).

[24] S. M. Albrecht, A. P. Higginbotham, M. Madsen, F. Kuemmeth, T. S. Jespersen, J. Nygård, P. Krogstrup, and C. M. Marcus, Nature (London) **531**, 206 (2016).

[25] J. Wiedenmann, E. Bocquillon, R. S. Deacon, S. Hartinger, O. Herrmann, T. M. Klapwijk, L. Maier, C. Ames, C. Brüne, C. Gould *et al.*, Nat. Commun. **7**, 10303 (2016).

[26] E. Bocquillon, R. S. Deacon, J. Wiedenmann, P. Leubner, T. M. Klapwijk, C. Brüne, K. Ishibashi, H. Buhmann, and L. W. Molenkamp, Nat. Nanotechnol. **12**, 137 (2017).

[27] B. E. Feldman, M. T. Randeria, J. Li, S. Jeon, Y. Xie, Z. Wang, I. K. Drozdov, B. Andrei Bernevig, and A. Yazdani, Nat. Phys. **13**, 286 (2017).

[28] K. Zhang, J. Zeng, Y. Ren, and Z. Qiao, Phys. Rev. B **96**, 085117 (2017).

[29] R. M. Lutchyn, E. P. A. M. Bakkers, L. P. Kouwenhoven, P. Krogstrup, C. M. Marcus, and Y. Oreg, Nat. Rev. Mater. **3**, 52 (2018).

[30] D. Wang, L. Kong, P. Fan, H. Chen, S. Zhu, W. Liu, L. Cao, Y. Sun, S. Du, J. Schneeloch, R. Zhong, G. Gu, L. Fu, H. Ding, and H.-J. Gao, Science **362**, 333 (2018).

[31] C. Chen, Q. Liu, T. Z. Zhang, D. Li, P. P. Shen, X. L. Dong, Z.-X. Zhao, T. Zhang, and D. L. Feng, Chin. Phys. Lett. **36**, 057403 (2019).

[32] M. Chen, X. Chen, H. Yang, Z. Du, X. Zhu, E. Wang, and H.-H. Wen, Nat. Commun. **9**, 970 (2018).

[33] T. Machida, Y. Sun, S. Pyon, S. Takeda, Y. Kohsaka, T. Hanaguri, T. Sasagawa, and T. Tamegai, Nat. Mater. **18**, 811 (2019).

[34] S. Zhu, L. Kong, L. Cao, H. Chen, M. Papaj, S. Du, Y. Xing, W. Liu, D. Wang, C. Shen *et al.*, Science **367**, 189 (2020).

[35] Q. Liu, C. Chen, T. Zhang, R. Peng, Y.-J. Yan, C.-H.-P. Wen, X. Lou, Y.-L. Huang, J.-P. Tian, X.-L. Dong *et al.*, Phys. Rev. X **8**, 041056 (2018).

[36] L. Kong, S. Zhu, M. Papaj, H. Chen, L. Cao, H. Isobe, Y. Xing, W. Liu, D. Wang, P. Fan *et al.*, Nat. Phys. **15**, 1181 (2019).

[37] P. Zhang, Z. Wang, X. Wu, K. Yaji, Y. Ishida, Y. Kohama, G. Dai, Y. Sun, C. Bareille, K. Kuroda *et al.*, Nat. Phys. **15**, 41 (2019).

[38] W. Liu, L. Cao, S. Zhu, L. Kong, G. Wang, M. Papaj, P. Zhang, Y.-B. Liu, H. Chen, G. Li *et al.*, Nat. Commun. **11**, 5688 (2020).

[39] M. Li, G. Li, L. Cao, X. Zhou, X. Wang, C. Jin, C.-K. Chiu, S. J. Pennycook, Z. Wang, and H.-J. Gao, Nature (London) **606**, 890 (2022).

[40] W. Liu, Q. Hu, X. Wang, Y. Zhong, F. Yang, L. Kong, L. Cao, G. Li, Y. Peng, K. Okazaki, T. Kondo, C. Jin, J. Xu, H.-J. Gao, and H. Ding, Quantum Front. **1**, 20 (2022).

[41] P. Bonderson, M. Freedman, and C. Nayak, Phys. Rev. Lett. **101**, 010501 (2008).

[42] P. Bonderson, M. Freedman, and C. Nayak, Ann. Phys. **324**, 787 (2009).

[43] S. Vijay and L. Fu, Phys. Rev. B **94**, 235446 (2016).

[44] T. Karzig, C. Knapp, R. M. Lutchyn, P. Bonderson, M. B. Hastings, C. Nayak, J. Alicea, K. Flensberg, S. Plugge, Y. Oreg *et al.*, Phys. Rev. B **95**, 235305 (2017).

[45] P. Bonderson, Phys. Rev. B **87**, 035113 (2013).

[46] H. Zheng, A. Dua, and L. Jiang, Phys. Rev. B **92**, 245139 (2015).

[47] H. Zheng, A. Dua, and L. Jiang, New J. Phys. **18**, 123027 (2016).

[48] A. Kitaev, Ann. Phys. **321**, 2 (2006).

[49] P. Bonderson, K. Shtengel, and J. K. Slingerland, Ann. Phys. **323**, 2709 (2008).

[50] J. K. Pachos, *Introduction to Topological Quantum Computation* (Cambridge University Press, Cambridge, 2012).

[51] S. H. Simon, *Topological Quantum* (Oxford University Press, Oxford, 2023).

[52] S. D. Sarma, M. Freedman, and C. Nayak, npj Quantum Inf. **1**, 15001 (2015).

[53] A. Tran, A. Bocharov, B. Bauer, and P. Bonderson, SciPost Phys. **8**, 091 (2020).

[54] T. Karzig, Y. Oreg, G. Refael, and M. H. Freedman, Phys. Rev. B **99**, 144521 (2019).

[55] See Supplemental Material at http://link.aps.org/supplemental/10.1103/PhysRevB.109.165302 for (A) correcting the undesired outcomes in detail; (B) measurement sequence of CZ gate; (C) associated with the other two qubit Clifford gates; (D) Majorana wave function; and (E) the detailed discussion of the concrete Majorana platform, which also includes Refs. [61–63].

[56] In more generic quantum circuits, there are usually Clifford gates and non-Clifford gates. One aspect to consider is that non-Clifford gates, which may not benefit from topological protection, can be susceptible to errors. The combination of Pauli correction [53], Clifford corrections and unforeseen errors from non-Clifford gates can lead to potential error evolution, such as non-Clifford correction, and propagation.

[57] N. H. Lindner, E. Berg, G. Refael, and A. Stern, Phys. Rev. X **2**, 041002 (2012).

[58] M. Cheng, Phys. Rev. B **86**, 195126 (2012).

[59] S. Plugge, A. Rasmussen, R. Egger, and K. Flensberg, New J. Phys. **19**, 012001 (2017).

[60] J. Alicea, Rep. Prog. Phys. **75**, 076501 (2012).

[61] A. Blais, R.-S. Huang, A. Wallraff, S. M. Girvin, and R. J. Schoelkopf, Phys. Rev. A **69**, 062320 (2004).

[62] J. Koch, T. M. Yu, J. Gambetta, A. A. Houck, D. I. Schuster, J. Majer, A. Blais, M. H. Devoret, S. M. Girvin, and R. J. Schoelkopf, Phys. Rev. A **76**, 042319 (2007).

[63] T. W. Larsen, M. E. Gershenson, L. Casparis, A. Kringhøj, N. J. Pearson, R. P. G. McNeil, F. Kuemmeth, P. Krogstrup, K. D. Petersson, and C. M. Marcus, Phys. Rev. Lett. **125**, 056801 (2020).